

Achieving a Strongly Temperature-Dependent Casimir Effect

Alejandro W. Rodriguez,¹ David Woolf,² Alexander P. McCauley,¹
Federico Capasso,² John D. Joannopoulos,¹ and Steven G. Johnson³

¹*Department of Physics, Massachusetts Institute of Technology, Cambridge, MA 02139*

²*Department of Applied Physics, Harvard University, Cambridge, MA 02139*

³*Department of Mathematics, Massachusetts Institute of Technology, Cambridge, MA 02139*

We propose a method of achieving large temperature T sensitivity in the Casimir force that involves measuring the stable separation between dielectric objects immersed in a fluid. We study the Casimir force between slabs and spheres using realistic material models, and find large $> 2\text{nm/K}$ variations in their stable separations (hundreds of nanometers) near room temperature. In addition, we analyze the effects of Brownian motion on suspended objects, and show that the average separation is also sensitive to changes in T . Finally, this approach also leads to rich qualitative phenomena, such as irreversible transitions, from suspension to stiction, as T is varied.

PACS numbers:

Casimir forces between macroscopic objects arise from thermodynamic electromagnetic fluctuations, which persist even in the limit of zero temperature due to quantum-mechanical effects (the Bose–Einstein distribution of the photon fluctuations) [1]. In most vacuum-separated geometries, such as parallel metal plates, the force is attractive and decaying as a function of plate–plate separation [1], becoming readily observable at micron and submicron separations. For a nonzero temperature T , the force is predicted to change as a consequence of the changing photon thermal distribution, but this change is typically negligible near room temperature and submicron separations [2, 3] and is only a few percent for ~ 100 K changes in T at $1\text{--}2\mu\text{m}$ separations where Casimir forces are barely observable [2–4]. Therefore, despite theoretical interest in these T effects [2, 5], it has proven difficult for experiments to unambiguously observe T corrections to the Casimir force [4]. Other attempts to measure T Casimir corrections have focused on nonequilibrium situations that differ conceptually from forces due purely to equilibrium fluctuations [6]. A clear experimental verification of a T Casimir correction would be important in order to further validate the foundation of Lifshitz theory for Casimir effects [2, 3].

In this letter, we propose a method for obtaining strongly temperature-dependent Casimir effects by exploiting geometries involving fluid-separated dielectric objects (with separations in the hundreds of nanometers). In fluid-separated geometries, the Casimir force can be repulsive [1, 7], and can even lead to stable suspensions of objects due to force-sign transitions from material dispersion [8, 9] or gravity [9, 10]. We show that, by a proper choice of materials/geometries, this stable separation d can depend dramatically on T (2 nm/K is easily obtainable), and there can even be transitions where d jumps discontinuously at some T . Essentially, a stable separation arises from a delicate cancellation of attractive and repulsive contributions to the force from fluctuations at different frequencies, and this cancellation is easily al-

tered or upset by the T corrections. This appears to be the first prediction of a strong T -dependent Casimir phenomenon at submicron separations where Casimir effects are most easily observed. We present the phenomenon in simple parallel-plate geometries, but we believe that the basic idea should extend to many other geometries and materials combinations that have yet to be explored. Finally, we also point out that the same systems that are strongly T -dependent can also be very sensitive to the precise details of the material dispersion at low frequencies, a property that we plan to exploit in the future.

The Casimir force between two bodies is a combination of fluctuations at all frequencies ω , and at $T = 0$ can be expressed as an integral $F(0) = \int_0^\infty f(\xi) d\xi$ over imaginary frequencies $\omega = i\xi$ [1]. The contributions $f(\xi)$ from each imaginary frequency are a complicated function of the geometry and materials, but they can be computed in a variety of ways, such as mean stress tensors and the fluctuation–dissipation theorem [7] (valid in fluids for subtle reasons [11, 12]) or via the Casimir energy [12]. At a finite T , this integral is replaced by a sum over “Matsubara frequencies” $2\pi n k T / \hbar = n \xi_T$ for integers n :

$$F(T) = \frac{2\pi k T}{\hbar} \left[\frac{f(0^+)}{2} + \sum_{n=1}^{\infty} f\left(\frac{2\pi k T}{\hbar} n\right) \right]. \quad (1)$$

Physically, this arises as a consequence of the $\coth(\hbar\omega/2kT)$ Bose–Einstein distribution of fluctuations at real frequencies—when one performs a contour integration in the upper-half complex- ω plane, the residues of the \coth poles at $\hbar\omega/2kT = ni\pi$ lead to the summation [4]. Mathematically, Eq. (1) corresponds exactly (including the $1/2$ factor for the zero-frequency contribution) to a trapezoidal-rule approximation to the $F(0)$ integral, which allows one to use the well-known convergence properties of the trapezoidal rule [13] to understand the magnitude of the T correction. In particular, the difference between the trapezoidal rule and the exact integral scales as $O(T^2)$ for smooth $f(\xi)$ with nonzero

derivative $f'(0)$ [2] (typical for Casimir forces between metals [3]). More specifically, $f(\xi)$ is exponentially decaying with a decay-length $2\pi c/a$ for some characteristic lengthscale a (e.g. the separation or size of the participating objects), while the discrete sum of Eq. (1) corresponds to a lengthscale given by the Matsubara wavelength $\lambda_T = 2\pi c/\xi_T = \hbar c/kT$, in which case one would expect the T correction to scale as $O(\lambda_T^2/a^2)$. Unfortunately, at $T = 300$ K, $\lambda_T \approx 7.6 \mu\text{m}$, which is why the T corrections are typically so small unless $a > 1 \mu\text{m}$ [2]. We cannot change the smoothness of $f(\omega)$ since it arises from the analyticity of the classical electromagnetic Green's function in the upper-half complex- ω plane [1], so the only way to obtain a larger T correction is to introduce a longer lengthscale Λ into the problem that dominates over other lengthscales such as the separation a . One way of achieving this is to make the $f(\xi)$ integrand *oscillatory* with an oscillation period $\Delta\xi \sim 2\pi c/\Lambda$ that is much shorter than the decay length $\sim 2\pi c/a$. Intuitively, discretizing an oscillatory integral induces much larger discretization effects than for a non-oscillatory integral, and this intuition can be formalized by a Fourier analysis of the convergence rate of the trapezoidal rule [13]. The question then becomes: how does one obtain an oscillatory Casimir integral?

One way to obtain oscillatory frequency contributions to the Casimir force is to employ a system where there are combinations of attractive and repulsive contributions. In particular, it is well known that the sign of $f(\xi)$ between two dielectric objects embedded in a fluid depends on the ordering of their dielectric functions at ξ [7, 14]:

$$\text{sgn}(f(\xi)) = \begin{cases} -1, & \varepsilon_1(i\xi) < \varepsilon_{\text{fluid}}(i\xi) < \varepsilon_2(i\xi) \\ 1, & \text{otherwise,} \end{cases} \quad (2)$$

where $+/-$ denotes an attractive/repulsive force. Since the Casimir force depends on the dielectric response of the participating objects over a wide range of ξ , from $\xi = 0$ all the way to $\xi \sim 2\pi c/a$ (where a is a characteristic lengthscale), the sign and magnitude of the total force at any given separation can be changed by a proper choice of material dispersion, leading to the possibility of obtaining Casimir equilibria between objects at multiple separations. This idea was recently exploited to demonstrate the possibility of obtaining stable nontouching configurations of dielectric objects amenable to experiments [9]. In this paper, for the purpose of achieving a strong T -dependence at short (submicron) separations, we search for materials or geometries with dielectric crossings occurring at sufficiently small $\xi = 2\pi c/\Lambda \sim \xi_T$, close to the room-temperature Matsubara-frequency scale ξ_T .

To begin with, we compute the Casimir force between semi-infinite slabs, computed via a generalization of the Lifshitz formula [19] that can handle multi-layer dielectric objects, with relative permittivities ε plotted in Fig. 1

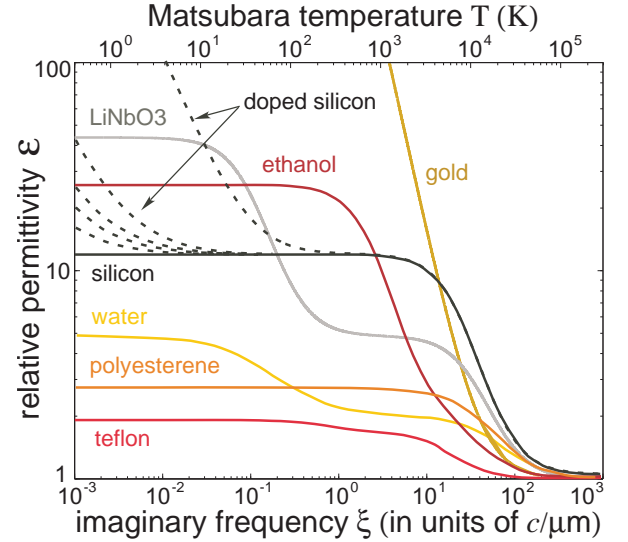


FIG. 1: Relative permittivity $\varepsilon(i\xi)$ of various materials as a function of imaginary frequency ξ (in units of $c/\mu\text{m}$) or “Matsubara” temperature $T = \hbar\xi/2\pi k_B$. Doped silicon corresponds (bottom to top) to doping density $\rho_d = \{1, 3, 5, 10, 10^2\} \times 10^{16}$, modeled via an empirical Drude model [15], as is gold [16]. Water, polystyrene, ethanol, teflon, and lithium niobate are all modeled via standard Lorentz-oscillator models [17].

as a function of imaginary frequency $i\xi$ (bottom axis) or “Matsubara temperature” $T = \hbar\xi/2\pi k$ (top axis). Figure 2 shows the equilibrium separation d_c (in units of μm) as a function of temperature $T \in (0, 400)$ K (in Kelvin) for some of the material combinations (solid/dashed lines correspond to stable/unstable equilibria), and demonstrates various degrees of T sensitivity. The previously studied [9] material combination of teflon/ethanol/silicon (data not shown) shows very little T -dependence: d_c varies $< 1\%$ over 400 K. More dramatic behavior is obtained for lithium niobate (LiNbO3) or doped silicon (doping density $\rho_d = \{1, 10, 100, 500, 10^3\} \times 10^{17}$), whose low- ξ ε crossings with ethanol lead to the desired oscillatory $f(\xi)$ in (1): the stable-equilibrium separation $d_c^{(s)}$ for both cases decreases by $> 2 \mu\text{m}$ over 400 K, and $\frac{d}{dT}d_c^{(s)} \approx -2 \text{ nm/K}$ near $T = 300$ K (where $d_c^{(s)} \sim 300\text{--}700 \text{ nm}$). The sign of $\frac{d}{dT}d_c^{(s)}$ comes from the increasing domination of the repulsive small- ξ (large-separation) contributions to $f(\xi)$ as T increases. Varying the silicon doping density dramatically changes the T dependence because it tunes the low- ξ silicon/ethanol ε crossing in Fig. 1. Doped-silicon exhibits another interesting behavior: d_c disappears at a critical temperature T_c (determined by ρ_d) due to a bifurcation between the stable/unstable equilibria. (T_c can be tuned not only by changing ρ_d but also by changing the LiNbO3 layer-thickness, here $\sim 50\text{nm}$.) Experimentally, such a bifurcation yields an *irreversible* transition from suspension

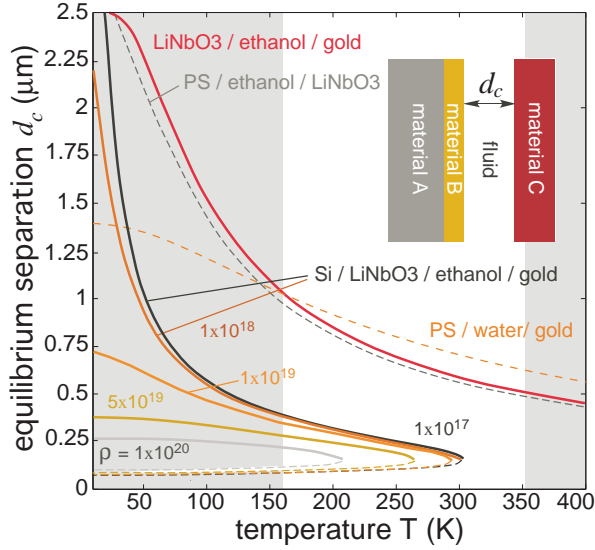


FIG. 2: Equilibrium separation d_c (in units of μm) as a function of temperature T (in Kelvin), for a geometry consisting of fluid-separated semi-infinite slabs (no gravity). The various curves correspond to d_c for various material combinations. Solid/dashed lines correspond to stable/unstable equilibria, and shaded regions are T where ethanol is non-liquid at 1 atm [18]. Doped-silicon is plotted for various doping densities $\rho_d = \{1, 10, 100, 500, 10^3\} \times 10^{17}$.

($T < T_c$) to stiction ($T > T_c$). Figure 2 also shows a small sample of the many other material possibilities. The shaded regions in Fig. 2 correspond to T above the boiling point (320 K) or below the freezing point (159 K) of ethanol at 1 atm [18].

The inclusion of gravity/buoyancy introduces another force into the system and leads to the possibility of additional phenomena, such as additional stable equilibria due to gravity/Casimir competition [9]. For example, Fig. 3 shows the equilibrium separations d_c of a polystyrene (PS) slab of thickness h in ethanol above a semi-infinite doped-silicon slab ($\rho_d = 1.1 \times 10^{15}$), including gravity (mass density $\rho_{\text{PS}} - \rho_{\text{ethanol}} = 0.264 \text{ g/cm}^3$ [18]). As in Fig. 2, d_c varies dramatically with T : $\frac{d}{dT}d_c \approx 1.2 \text{ nm/K}$ near $T = 300 \text{ K}$. Gravity becomes increasingly important as h grows: compared to $h = 0$ (leftmost line), it creates an additional stable equilibrium (solid lines) at large d_c (hundreds of nm) where the downward gravity dominates. With gravity, there are three stable/unstable bifurcations instead of two, leading to three critical temperatures where qualitative transitions occur: T_g refers to the temperature of the topmost bifurcation, created by gravity, and the other two temperatures are labeled T_1 ($\approx 100 \text{ K}$) and T_2 ($\approx 180 \text{ K}$). If $T_g < T_1$ ($h < 40 \text{ nm}$), there exists an irreversible transition from suspension to stiction as T is decreased below T_g . If $T_1 < T_g < T_2$, there are two irreversible transitions from suspension to suspension (smaller d_c) to stiction as T is lowered from $T > T_g$ to $T < T_1$ starting in the large-

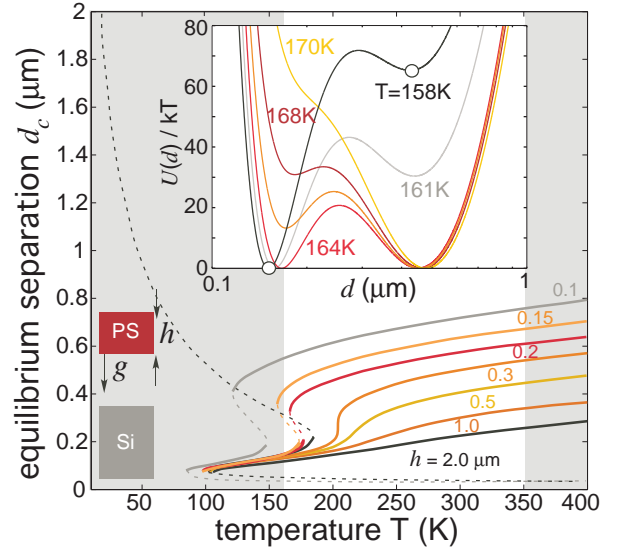


FIG. 3: Equilibrium position d_c (in units of μm) of a semi-infinite polystyrene (PS) slab immersed in ethanol (shaded $T = \text{non-liquid}$) and suspended against gravity by a repulsive Casimir force exerted by a doped-silicon (Si) slab. The solid/dashed lines correspond to stable/unstable d_c , and each color represents a different value of PS slab-thickness h (in units of μm). The inset shows the magnitude of the total energy $U_T(d)$ (in units of $k_B T$) as a function of d for $h = 150 \text{ nm}$, at various T .

d_c equilibrium. Finally, when $T_g \rightarrow T_2$ ($h \approx 300 \text{ nm}$) the two stable equilibria merge and only the T_1 bifurcation remains. Perhaps most interestingly, when this merge occurs the slope $\frac{d}{dT}d_c$ can be made arbitrarily large but finite, corresponding to an arbitrarily large (but reversible) temperature dependence. For example, $\Delta d_c \approx 130 \text{ nm}$ for a small change $\Delta T \approx 5 \text{ K}$ around T_2 , for $h = 300 \text{ nm}$.

In a real experiment, the situation is further complicated by Brownian motion, which will cause the separation to fluctuate around stable equilibria and will also lead to random transitions between equilibria [20]. In the example of Fig. 3, the attractive interaction at small separations means that there is a nonzero probability that the slabs will fluctuate past the unstable-equilibrium energy barrier ΔU_T into stiction, but the rate of such a transition decreases proportional to $\exp(-\Delta U_T/k_B T)$ [20]—here, assuming a $50 \times 50 \mu\text{m}^2$ PS slab, $\Delta U_T/k_B T \approx 10^4$, so the stiction rate is negligible. The energy landscape $U_T(d)/k_B T$ is plotted for several cases in the inset to Fig. 3: the general prediction of experimental observations involves a viscosity-damped Langevin process [20] that is beyond the scope of this paper to model, but by choosing T one can make the potential barrier between the two stable equilibria arbitrarily small and therefore should be able to reach an experimental regime in which “hopping” is observable.

Alternatively, we consider a simpler example system with only a single stable equilibrium and a single degree

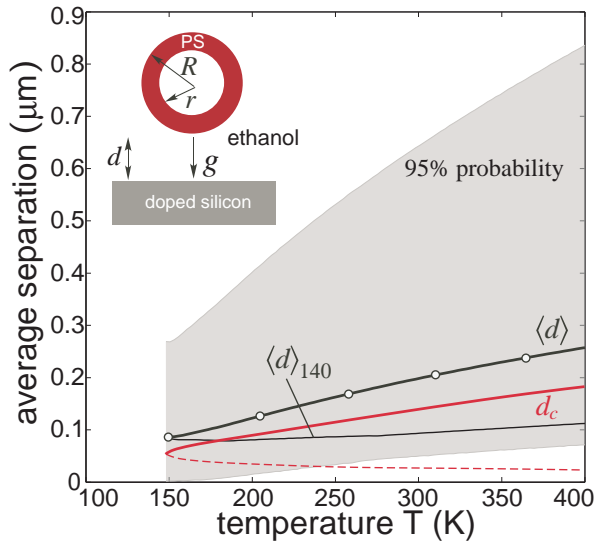


FIG. 4: Average separation $\langle d \rangle$ (circles) and equilibrium separation d_c (red line), in units of μm , vs. temperature T (in Kelvin), for a geometry consisting of a fluid-separated hollow PS sphere of inner/outer radius $r/R = 3.2/5 \mu\text{m}$ suspended in ethanol against gravity by a doped-silicon slab and subject to Brownian motion. Shaded region indicates where sphere is found with 95% probability. The thin black line is the average $\langle d \rangle_{140}$ if the Casimir energy at 140 K is used instead of the true temperature-dependent energy landscape.

of freedom: a hollow PS sphere (experimentally available at similar scales [21]), filled with ethanol, of inner/outer radius $r/R = 3.2/5 \mu\text{m}$ suspended in ethanol above a doped-silicon ($\rho_d = 1.1 \times 10^{15}$) substrate, shown on the inset of Fig. 4. (To compute the Casimir energy in this system, we employ a simple PFA approximation that is sufficiently accurate for our purpose. Here, for $d \approx 500$ nm, the exact energy is $\approx 85\%$ of the PFA energy.) For this example, in Fig. 4 we plot the mean surface-surface separation $\langle d \rangle \sim \int dz z \exp[U_T(z)/k_B T]$ (determined only by the energy landscape and the Boltzmann distribution [20]), corresponding to an experiment averaging d over a long time, along with a confidence interval (shaded region) indicating the range of d where the particle is found with 95% probability. The sphere experiences an attractive interaction at small separations, but again we find that the unstable-equilibrium energy barrier is sufficiently large ($\Delta U/k_B T \approx 50$) to prevent stiction for T near 300 K. As T varies, two factors affect $\langle d \rangle$: the T -dependence of the Casimir energy $U_T(z)$, and the explicit $k_B T$ in the Boltzmann factor. To distinguish these two effects, we also plot (thin black line) $\langle d \rangle_{140} \sim \int dz z \exp[U_{140}(z)/k_B T]$ where the $T = 140$ K (bifurcation point) Casimir energy is used at all temperatures. Comparing $\langle d \rangle$ with $\langle d \rangle_{140}$, it is evident that most of the positive-slope T dependence of $\langle d \rangle$ (≈ 0.8 nm/K around 300 K) is due to U_T , and therefore $\langle d \rangle$ offers a direct measure of the Casimir-energy T dependence.

Experimentally, measuring hundreds of nm changes in separation over tens or hundreds of Kelvins appears very feasible, perhaps even easier than traditional measurements of Casimir forces. (In a fluid, static-charge effects can be neutralized by dissolving electrolytes in the fluid [14], which also have the added benefit of significantly reducing/increasing the freezing/boiling point of the fluid [18].) Such temperature-dependent suspensions may even have practical applications in microfluidics. We believe that the examples shown in this letter only scratch the surface of the possible temperature/dispersion effects that can be obtained in Casimir-suspension systems. Not only are there many other possible materials and geometries to explore in the fluid context (along with more detailed calculation of the Brownian dynamics), and by no means are the effects shown here the maximum possible, but similar principles should apply in other systems exhibiting competing attractive/repulsive Casimir-force contributions.

This work was supported by the Army Research Office through the ISN under Contract No. W911NF-07-D-0004, by US DOE Grant No. DE-FG02-97ER25308, and by the Defense Advanced Research Projects Agency (DARPA) under contract N66001-09-1-2070-DOD.

-
- [1] E. M. Lifshitz and L. P. Pitaevskii, *Statistical Physics: Part 2* (Pergamon, Oxford, 1980).
 - [2] K. A. Milton, Journal of Physics A: Mathematical and General **37**, R209 (2004).
 - [3] J. S. Hoye, I. Brevik, J. B. Aarseth, and K. A. Milton, J. Phys. A: Math. Gen. **39**, 6031 (2006).
 - [4] S. K. Lamoreaux, Phys. Rev. Lett. **78**, 5 (1997). M. Bostrom and B. E. Sernelius, Phys. Rev. Lett. **84**, 4757 (2000). M. Bordag, B. Geyer, G. L. Klimchitskaya, and V. M. Mostepanenko, Phys. Rev. Lett. **85**, 503 (2000).
 - [5] V. S. Bentsen, R. Herikstad, S. Skriudalen, I. Brevik, and J. S. Hoye, J. Phys. A: Math. Gen. **38** (2005). V. A. Yampol'skii, S. Savel'ev, Z. A. Mayselis, S. S. Apostolov, and F. Nori, Phys. Rev. Lett. **101**, 096803 (2008). A. Weber and H. Gies, arXiv:1003.0430 (2010).
 - [6] J. M. Obrecht, R. J. Wild, M. Antezza, L. P. Pitaevskii, S. Stringari, and E. A. Cornell, Phys. Rev. Lett. **98**, 063201 (2007).
 - [7] I. E. Dzyaloshinskii, E. M. Lifshitz, and L. P. Pitaevskii, Adv. Phys. **10**, 165 (1961).
 - [8] A. W. Rodriguez, J. Munday, D. Davlit, F. Capasso, J. D. Joannopoulos, and S. G. Johnson, Phys. Rev. Lett. **101**, 190404 (2008).
 - [9] A. W. Rodriguez, A. P. McCauley, D. Woolf, F. Capasso, J. D. Joannopoulos, and S. G. Johnson, arXiv:0912.2243 (2010).
 - [10] A. P. McCauley, A. W. Rodriguez, J. D. Joannopoulos, and S. G. Johnson, Phys. Rev. A **81**, 012119 (2010).
 - [11] L. P. Pitaevskii, Phys. Rev. A **73**, 047801 (2006).
 - [12] K. Milton, J. Wagner, P. Parashar, and I. Brevik, arXiv:1001.4163 (2010).

- [13] J. P. Boyd, *Chebyshev and Fourier Spectral Methods* (Dover, New York, 2001), 2nd ed.
- [14] J. N. Munday and F. Capasso, Phys. Rev. A **78**, 032109 (2008).
- [15] L. Duraffourg and P. Andreucci, Phys. Lett. A **359**, 406 (2006).
- [16] L. Bergstrom, Adv. Colloid and Interface Science **70**, 125 (1997).
- [17] J. Mahanty and B. W. Ninham, *Dispersion forces* (Academic London, 1976).
- [18] D. G. Friend and M. L. Hiber, Int. J. Thermophys. **15** (1994).
- [19] M. S. Tomaš, Phys. Rev. A **66**, 052103 (2002).
- [20] H. Risken, *The Fokker-Planck Equation: Methods of Solution and Applications* (Springer-Verlag, Heidelberg, New York, 1996).
- [21] D. L. Wilcox, M. Berg, T. Bernat, D. Kellerman, and J. K. Cochran, *Hollow and Solid Spheres and Microspheres: Science and Technology Associated with Their Fabrication and Application*, vol. 372 (Society Symposium Proceedings, 1995).